TRPC3-mediated Ca2+ influx contributes to Rac1-mediated production of reactive oxygen species in MLP-deficient mouse hearts

Kitajima, Naoyuki
Department of Pharmacology and Toxicology, Graduate School of Pharmaceutical Sciences, Kyushu University

Watanabe, Kunihiro
Department of Pharmacology and Toxicology, Graduate School of Pharmaceutical Sciences, Kyushu University

Morimoto, Sachio
Department of Clinical Pharmacology, Graduate School of Medical Sciences, Kyushu University

Sato, Yoji
Division of Cellular and Gene Therapy Products, National Institute of Health Sciences

他

出版情報：Biochemical and Biophysical Research Communications. 409 (1), pp.108-113, 2011-05-27. Elsevier
バージョン：

TRPC3-mediated Ca^{2+} influx contributes to Rac1-mediated production of reactive oxygen species in MLP-deficient mouse hearts

Naoyuki Kitajima[1], Kunihiro Watanabe[1], Sachio Morimoto[2], Yoji Sato[3], Shigeki Kiyonaka[4], Masahiko Hoshijima[5], Yasuhiro Ikeda[6], Michio Nakaya[1], Tomomi Ide[7], Yasuo Mori[4], Hitoshi Kurose[1] and Motohiro Nishida[1*]

[1]Department of Pharmacology and Toxicology, Graduate School of Pharmaceutical Sciences, Kyushu University, Fukuoka 812-8582, Japan

[2]Department of Clinical Pharmacology, Graduate School of Medical Sciences, Kyushu University, Fukuoka 812-8582, Japan

[3]Division of Cellular and Gene Therapy Products, National Institute of Health Sciences, Tokyo 158-8501, Japan

[4]Laboratory of Molecular Biology, Department of Synthetic Chemistry and Biological Chemistry, Graduate School of Engineering, Kyoto University, Kyoto 615-8510, Japan

[5]Department of Medicine, Division of Cardiology, University of California San Diego, La Jolla, CA 92093-0734, USA

[6]Division of Cardiology, Department of Medicine and Clinical Science, Yamaguchi University Graduate School of Medicine, Yamaguchi 755-8505, Japan.

[7]Department of Cardiovascular Medicine, Graduate School of Medical Sciences, Kyushu University, Fukuoka 812-8582, Japan.

*Corresponding author:

Motohiro Nishida, Ph.D.

Department of Pharmacology and Toxicology, Graduate School of Pharmaceutical Sciences, Kyushu University, 3-1-1 Maidashi, Higashi-ku, Fukuoka, Fukuoka 812-8582, Japan. E-mail: nishida@phar.kyushu-u.ac.jp. Tel and Fax: +81-92-642-6878.

E-mail address of each author:

Naoyuki Kitajima: nkitajima2012@gmail.com

Satoshi Morimoto: morimoto@med.kyushu-u.ac.jp

Kunihiro Watanabe: kunihirowatanabe1984@hotmail.com

Yoji Sato: yoji@nihs.go.jp

Shigeki Kiyonaka: kiyonaka@sbchem.kyoto-u.ac.jp

Masahiko Hoshijima: mhoshijima@ucsd.edu

Yasuhiro Ikeda: ysikeda@yamaguchi-u.ac.jp

Michio Nakaya: nakaya@phar.kyushu-u.ac.jp

Tomomi Ide: tomomi_i@cardiol.med.kyushu-u.ac.jp

Yasuo Mori: mori@ sbchem.kyoto-u.ac.jp

Hitoshi Kurose: kurose@phar.kyushu-u.ac.jp

Title characters: 121 (incl. space),

Abstract: 206 words

Total words: 4,585 words

Figures: 4

Tables: 2

Abbreviations

Ang, angiotensin; AT_1R, Ang type1 receptor; βAR, β adrenergic receptor; βARK, βAR kinase; βARK-ct, carboxyl-terminal region of βARK (βARK inhibitor); CaMKII, Ca^{2+}/calmodulin-dependent kinase II; DAG, diacylglycerol; DCF, dichlorofluorescein; DCM, dilated cardiomyopathy; DHE, dihydroethidium; DPI, diphenyleneiodonium; 4-HNE, 4-hydroxy-2-nonenal; LV, left ventricle; MLP, muscle LIM protein; LTCCs, L-type Ca^{2+} channels; NFAT, nuclear factor of activated T cells; Nox; NADPH oxidase; OAG, 1-oleoyl-2-acetyl-*sn*-glycerol; PKC, protein kinase C; pyrazole-3 (Pyr3), ethyl-1-(4-(2,3,3-trichloroacrylamide)phenyl)-5-(trifluoromethyl)-1H-pyrazole-4-carbox ylate; ROS, reactive oxygen species; RIRR, ROS-induced ROS release; TRP, transient receptor potential; TRPC, TRP canonical.

Abstract

Dilated cardiomyopathy (DCM) is a myocardial disorder that is characterized by dilation and dysfunction of the left ventricle (LV). Accumulating evidence has implicated aberrant Ca^{2+} signaling and oxidative stress in the progression of DCM, but the molecular details are unknown. In the present study, we report that inhibition of the transient receptor potential canonical 3 (TRPC3) channels partially prevents LV dilation and dysfunction in muscle LIM protein-deficient (MLP (-/-)) mice, a murine model of DCM. The expression level of TRPC3 and the activity of Ca^{2+}/calmodulin-dependent kinase II (CaMKII) were increased in MLP (-/-) mouse hearts. Acitivity of Rac1, a small GTP-binding protein that participates in NADPH oxidase (Nox) activation, and the production of reactive oxygen species (ROS) were also increased in MLP (-/-) mouse hearts. Treatment with pyrazole-3, a TRPC3 selective inhibitor, strongly suppressed the increased activities of CaMKII and Rac1, as well as ROS production. In contrast, activation of TRPC3 by 1-oleoyl-2-acetyl-*sn*-glycerol (OAG), or by mechanical stretch, induced ROS production in rat neonatal cardiomyocytes. These results suggest that up-regulation of TRPC3 is responsible for the increase in CaMKII activity and the Nox-mediated ROS production in MLP (-/-) mouse cardiomyocytes, and that inhibition of TRPC3 is an effective therapeutic strategy to prevent the progression of DCM.

Keywords: transient receptor potential channel, muscle LIM protein, dilated cardiomyopathy, Rac, reactive oxygen species.

Introduction

Dilated cardiomyopathy (DCM), a poorly understood disorder in which the LV chambers enlarge, is the most common causes for congestive heart failure [1]. Heart failure resulting from DCM is a principal cause of death and disability in children and young adults. Despite recent progress in the treatment of heart failure, the only meaningful treatment for DCM is cardiac transplantation. Although most cases of DCM develop as a consequence of specific inflammatory, metabolic or toxic insults [2], 25-35% of DCM cases are caused by genetic mutations [3-5]. Affected genes encode proteins that function in the Ca^{2+} regulatory system, the contractile/cytoskeltal apparatus, or reside at a sarcomeric Z-disc. One of the Z-disc proteins that has been implicated in DCM etiology is the muscle LIM protein (MLP) [6-8]. MLP interacts with telethonin, a titin-interacting protein, to form a component of the mechanical stretch apparatus [8], and genetic ablation of MLP in mice causes age-related DCM, which closely resembles human DCM [8, 9]. Thus, MLP deficient (MLP (-/-)) mice are commonly employed as a murine DCM model system. Since genetic ablation of angiotensin (Ang) II type1 receptor (AT_1R) or overexpression of the carboxyl-terminal region of the β adrenergic receptor (βAR) kinase (βARK-ct) attenuates the progression of heart failure in MLP (-/-) mice [10, 11], βAR and AT_1R signalings are thought to participate in the progression of heart failure in MLP (-/-) mice.

Abnormal Ca^{2+} metabolism and production of ROS have been implicated in the progressive deterioration of heart failure [12-14]. For example, activation of CaMKIIδ causes p53 accumulation and cardiomyocyte apoptosis in DCM [13]. In contrast, $p47^{phox}$, a Nox subunit, and the small GTP-binding protein Rac1, are up-regulated and

oxygen free radical release is increased in human LV myocardium from patients with DCM [14]. Furthermore, oxidative stress inactivates calcineurin, a Ca^{2+}-dependent protein phosphatase that mediates cardiac hypertrophy, indicating the functional cross-talk between Ca^{2+} signaling and ROS signaling [12]. Although both Ca^{2+} and ROS evidently play key roles in the progression of heart failure, their upstream regulator(s) remain elusive.

Transient receptor potential (TRP) family proteins, first described in a *Drosophila* visual transduction mutation *trp*, comprise 28 mammalian cation channels expressed in almost every tissue [15-17]. Among them, canonical TRP subfamily (TRPC) proteins have been up-regulated in hypertrophied and failing hearts [17-20]. TRPC channels were originally proposed as store-operated channels activated by Ca^{2+} depletion of stores, while closely related TRPC3, TRPC6, and TRPC7 showed activation sensitivity to the membrane-delimited action of diacylglycerol (DAG). In particular, TRPC1, TRPC3 and TRPC6 proteins participate in agonist-induced cardiomyocyte hypertrophy through activation of Ca^{2+}-dependent calcineurin/nuclear factor of activated T cells (NFAT) signaling pathways [18-20]. We have reported that TRPC3 and TRPC6 channels mediate the Ang II-induced cardiomyocyte hypertrophy *in vitro* and pressure overload-induced cardiac hypertrophy *in vivo* [21, 22]. The TRPC3/6-mediated cation influx induces membrane depolarization, followed by an increase in the frequency of Ca^{2+} transients evoked by voltage-dependent Ca^{2+} influx-induced Ca^{2+} release, leading to NFAT activation in rat cardiomyocytes [21]. However, calcineurin/NFAT signaling is apparently desensitized in MLP (-/-) mouse hearts, as MLP is essential for mechanical stretch-induced NFAT activation through anchorage of calcineurin at the Z-disc [23]. Therefore, it is unknown whether

TRPC-mediated Ca^{2+} signals are involved in the progression of heart failure in MLP (-/-) mice.

In the present study, we examine the effects of a selective TRPC3 inhibitor, pyrazole-3 (Pyr3) [22], in the progression of DCM using the MLP (-/-) mouse model. We demonstrate that TRPC3-mediated Ca^{2+} signals are increased in MLP (-/-) mouse hearts, and Pyr3 potently inhibits LV dysfunction, CaMKII activation and ROS production. The inhibitory effect of Pyr3 on LV dysfunction is apparently small compared to the pronounced effects on CaMKII activation and ROS production, indicating that TRPC3 only plays a complementary role in the progression of DCM. However, our findings suggest that TRPC3 blockade is a therapeutic strategy for preventing DCM.

2. Materials and Methods

2.1 Animals and drug treatment

The basal cardiomyopathic phenotype of MLP (-/-) mice was described previously [7, 8]. Wild type littermates (MLP (+/+)) served as controls for all studies. A mini osmotic pump (Alzet) filled with pyrazole 3 (Pyr3), a selective inhibitor of TRPC3, or polyethylene glycol 300 (vehicle) was implanted intraperitoneally into 5-week-old mice, and Pyr3 (0.1 mg/kg/day) was continuously administered for 3 weeks. All animal care procedure and experiments were approved by the guidelines of Kyushu University.

2.2 Transthoracic echocardiography and cardiac catheterization

Echocardiography was performed in anesthetized mice (50 mg/kg pentobarbital sodium) by using Nemio-XG echocardiograph (TOSHIBA) equipped with a 14MHz transducer. A 1.4 French micronanometer catheter (Millar Instruments, Houston, TX) was inserted into the left carotid and advanced retrograde into the LV. Hemodynamic measurements were recorded when heart rate was stabilized within 500 ± 10 beats/min.

2.3 Histological analysis of mouse hearts

The paraffin-embedded LV sections (5 μm in thickness) were stained with hematoxylin and eosin (H&E) or picrosirius red, and cell-sectional area (CSA) of cardiomyocytes and collagen volume fraction (CVF) of LV sections were analysed using BZ-II analyzer (Keyence) [24].

2.4 Isolation of cardiomyocytes and siRNA treatment

Rat neonatal cardiomyocytes were prepared as described previously [25]. For knockdown of rat TRPC3 proteins, cells were transfected with siRNA (100 nM) for TRPC3 using lipofectamine2000 for 72 h [26]. Adult mouse cardiomyocytes were isolated from 8-week-old mouse hearts as described previously [5].

2.5 Real time PCR, pulldown assay, and Western blot analysis

RNA extraction, real time RT-PCR and Rac pulldown assay were performed as described previously [24]. Hearts were homogenized in RIPA buffer (pH 8.0) containing 0.1% SDS, 0.5% sodium deoxycholate, 1% NP-40, 150 mM NaCl, 50 mM Tris-HCl, and protease inhibitor cocktail (Nacalai). Supernatants (10 μg) were fractionated by SDS-PAGE gel, and expression levels of endogenous proteins were detected by antibodies raised against ACE (1/10000, R&D systems), Periostin (1/10000, R&D systems), Rac1 (1/1000, BD Bioscience), CaMKII (1/1000, Santa Cruz), phospho-CaMKII (Thr286) (1/1000, Cell Signaling) and GAPDH (1/3000, Santa Cruz). Membrane fractions (10 μg) were isolated using Proteoextract transmembrane protein extraction kit (Novagen) to detect TRPC1, TRPC3, TRPC5, TRPC6 and TRPC7 proteins using respective TRPC antibodies (1/2000, Alomone). Proteins were visualized with chemiluminescent detection of antibodies conjugated with horseradish peroxidase (ECL plus, Perkin Elmer). The optical density of the film was scanned and measured with Scion Image Software.

2.6 Measurement of ROS production and intracellular Ca^{2+} concentration

The paraffin-embedded LV sections were stained with anti-4-hydroxy-2-nonenal (4-HNE) antibody (1/500: JaICA, Nikken Seil Co., Ltd.).

The 4-HNE adducts were visualized with Alexa Fluor 546 anti-mouse IgG antibody (1/1000, Molecular Probes). Superoxide production in the heart was measured using dihydroethidium (DHE) [27]. Hearts were solidified with liquid nitrogen and sectioned in 10 μm thickness using Cryostat (Leica, CM1100). The LV sections were incubated with DHE (100 μM) at room temperature for 5 min. After washing the LV sections with PBS, digital photographs were taken at x60 magnification using confocal microscopy (FV10i, Olympus), and 5 regions selected at random for each specimen of the heart. The average intensity was analyzed using MetaMorph Software. Measurement of intracellular Ca^{2+} concentration ($[Ca^{2+}]_i$) in adult mouse cardiomyocytes was performed using fura-2 [26]. Production of ROS in rat neonatal cardiomyocytes was measured using 2′,7′-dichlorofluorescein diacetate ($DCFH_2DA$) and DHE [27]. Cells plated on laminin-coated silicone rubber culture dishes were loaded with $DCFH_2DA$ (10 μM) at 37 °C for 10 min. The DCF fluorescence or fura-2 fluorescence at an emission wavelength of 510 nm was observed at room temperature by exciting DCF at 488 nm or exciting fura-2 at 340 nm and 380 nm using a video image analysis system (Aquacosmos, Hamamatsu Photonics).

2.7 Statistical Analysis

The results are shown as means ± S.E.M. All experiments were repeated at least three times. Statistical comparisons were made with two-tailed Student's *t*-test or one way analysis of variance followed by the Student-Newman-Keuls procedure with significance imparted at $P < 0.05$.

3. Results

3.1. Increase in TRPC3-mediated Ca^{2+} signals in MLP (-/-) mouse hearts.

Compared with MLP (+/+) mouse hearts, the expression levels of TRPC3 and TRPC6 proteins, but not TRPC1, TRPC5, and TRPC7, were significantly increased in MLP (-/-) mouse hearts (Figure 1A). Treatment of isolated MLP (+/+) mouse cardiomyocytes with OAG induced a Ca^{2+} influx-mediated increase in $[Ca^{2+}]_i$. This $[Ca^{2+}]_i$ increase was completely suppressed by the addition of Pyr3 (Figure 1B). The OAG-induced maximal $[Ca^{2+}]_i$ increase was markedly enhanced in MLP (-/-) mouse cardiomyocytes (Figure 1C), indicating that up-regulation of TRPC3 enhances DAG-mediated Ca^{2+} influx. NFAT and CaMKII are two major downstream effectors of Ca^{2+}/calmodulin-mediated cardiac hypertrophy [17]. The CaMKII activity was increased in MLP (-/-) mouse hearts (Figure 1D). This CaMKII activation was significantly suppressed by Pyr3 treatment. These results suggest that up-regulation of TRPC3 contributes to Ca^{2+} influx-dependent CaMKII activation in MLP (-/-) mouse hearts.

3.2. Inhibition of TRPC3 attenuates LV dilation and dysfunction.

Both LV wall thickness and LV function were markedly reduced in 8-week-old MLP (-/-) mouse hearts (Table 1 and 2). Treatment of MLP (-/-) mice with Pyr3 significantly attenuated the progression of LV dilation and dysfunction. Inhibition of TRPC3 also reduced the increase in heart weight and cardiomyocyte hypertrophy (Figure 2A-C) and the increases in mRNAs of hypertrophy-related markers (β-myosin heavy chain (βMHC), α-skeletal muscle actin (αSKA) and Ang converting enzyme (ACE)) (Figure 2D). We previously reported that cardiac hypertrophy and fibrosis are

independently regulated by two heterotrimeric GTP-binding proteins [24]. Therefore, we next examined whether inhibition of TRPC3 suppresses cardiac fibrosis in MLP (-/-) mice. Collagen deposition in the interstitial area was markedly increased in MLP (-/-) hearts, and this fibrosis was suppressed by Pyr3 treatment (Figure 3A, B). Pyr3 also suppressed the increase in expression of fibrosis-inducible proteins (ACE and periostin) in MLP (-/-) mouse hearts (Figure 3C). These results suggest that inhibition of TRPC3 attenuates the development of cardiac hypertrophy and fibrosis in MLP (-/-) mice.

3.3. TRPC3-mediated Ca^{2+} influx contributes to ROS production

It is generally thought that oxygen free radical release is increased in the failing heart and oxidative stress is a major cause of the progression of heart failure [12, 14]. Up-regulation of TRPC3 channels participate in CaMKII activation in MLP (-/-) mouse hearts, and it has been reported that Ca^{2+} influx is required for Nox-mediated ROS production [28, 29]. Therefore, we examined whether TRPC3-mediated Ca^{2+} influx regulates ROS production in DCM. The expression level of 4-HNE adducts and superoxide production were markedly increased in MLP (-/-) mouse hearts (Figure 4A, B). These ROS accumulations were completely suppressed by Pyr3. Mitochondria and Nox are two major sources of ROS in the heart. The heart expresses two Nox isoforms: Nox2 and Nox4 [30, 31], and up-regulation of either isoform has been reported to induce mitochondrial dysfunction in the heart [14, 31]. The Nox2 activity is predominantly regulated by Rac, $p47^{phox}$, $p67^{phox}$, and $p22^{phox}$, while Nox4 is constitutively activated [32]. In addition, Rac1 has been implicated in the progression of DCM [14]. Although Nox2 and Nox4 mRNA levels were not increased in MLP (-/-) mouse hearts (data not shown), the expression and activity of Rac1 were markedly

increased (Figure 4C). Treatment with Pyr3 significantly suppressed Rac1 activation without affecting total Rac1 protein levels. These results suggest that up-regulation of TRPC3 contributes to Rac1-mediated ROS production in MLP (-/-) mouse hearts. We further examined whether activation of TRPC3 actually induces ROS production in rat neonatal cardiomyocytes. We recently reported that mechanical stretch induces a Ca^{2+} response through activation of TRPC3/6 channels [26]. Mechanical stretch of cardiomyocytes gradually increased DCF fluorescence intensity (Figure 4D). This ROS production was significantly suppressed by Pyr3 or knockdown of TRPC3. Treatment with OAG also induced superoxide production, and the DHE accumulation was reduced by TRPC3 knockdown or by pretreatment with Pyr3 or diphenyleneiodonium (DPI), a Nox inhibitor (Figure 4E, F). Furthermore, the OAG-induced superoxide production was inhibited by the elimination of extracellular Ca^{2+}. These results suggest that TRPC3-mediated Ca^{2+} influx mediates ROS production through Nox activation in rodent cardiomyocytes.

4. Discussion

Several reports have suggested the involvement of TRPC up-regulation in the development of cardiac hypertrophy *in vivo* [17-20]. On the other hand, DCM is believed to represent a maladaptive response of the heart in a late stage of heart failure. We first demonstrated that TRPC3 channels participate in the progression of DCM. In the DCM mouse model, the up-regulation of TRPC3 increases not only cardiomyocyte Ca^{2+}-dependent CaMKII activity, but also ROS production. TRPC channels have two functions: to act as receptor-activated or mechanical stretch-activated cation channels in cardiomyocytes, and to act as a protein scaffold at the plasma membrane to control the amplification and co-ordination of receptor signaling [16, 33, 34]. We previously reported that TRPC3 interacts with phospholipase C and protein kinase C (PKC), leading to sustained activation of an extracellular signal-regulated kinase induced by receptor stimulation in B lymphocytes [33, 34]. Activation of PKC contributes to Nox2 activation through phosphorylation of the $p47^{phox}$ subunit [32]. In addition, we found that TRPC3-mediated Ca^{2+} influx also contributes to Rac1 activation in MLP (-/-) mouse hearts (Figure 4). Although the molecular mechanism underlying activation of Rac1 by Ca^{2+} is still unclear, our results strongly suggest that TRPC3-mediated Ca^{2+} influx controls Nox-dependent ROS production in rodent cardiomyocytes.

Oxidative stress plays a critical role in the progression of DCM, and the major source of ROS production in the heart is mitochondria. Based on the results that the increase in ROS production was associated with an increase in Rac activity in MLP (-/-) mouse hearts, and that the Nox inhibitor suppressed TRPC3-mediated superoxide production in rat cardiomyocytes (Figure 4), Nox may be a primary source of ROS production. ROS have been reported to induce mitochondrial superoxide production,

by a phenomenon reported as ROS-induced ROS release (RIRR) [35, 36]. Thus, TRPC3-mediated Ca^{2+} influx in rodent cardiomyocytes may initially induce Nox-dependent ROS production, with the subsequent induction of an oxygen burst through RIRR-mediated ROS production.

Previous reports have shown that ablation of AT_1R or expression of βARK-ct attenuates LV dysfunction in MLP (-/-) mice. We also reported that TRPC3/TRPC6 mediates Ang II-induced cardiomyocyte hypertrophy [21], suggesting that AT_1R works upstream of TRPC3 in MLP (-/-) mouse hearts. In contrast, βARK-ct inhibits βARK1-mediated β_1AR internalization through sequestration of the βγ subunit (Gβγ) released from the α_s subunit of G proteins coupled to β_1AR. However, inhibition of TRPC3 does not affect β_1AR-mediated Ca^{2+} signaling in rat cardiomyocytes (unpublished data). As βARK is activated by $G\alpha_q$-mediated PKC activation in rat cardiomyocytes [37], one explanation is that TRPC3 contributes to PKC-mediated βARK activation downstream of AT_1R signaling in the heart [34].

Both Ca^{2+}/calmodulin-dependent calcineurin and CaMKII function as key mediators in the development of cardiac hypertrophy [38, 39]. Cardiomyocyte-specific overexpression of the constitutively active mutant of NFAT causes cardiac hypertrophy, whereas expression of calcineurin or CaMKII causes cardiomyopathy [13, 40]. Although calcineurin/NFAT signaling may participate in the development of hypertrophy, CaMKII may participate in the development of heart failure. Since the inhibition of TRPC3 suppresses both calcineurin/NFAT and CaMKII signaling pathways in cardiomyocytes, our findings strongly suggest TRPC3 channels as a putative therapeutic target for the treatment of heart failure.

Acknowledgements

This study was supported by grants from Grant-in-Aid for Scientific Research on Innovative Areas (M. Nishida); from the Ministry of Education, Culture, Sports, Science, and Technology of Japan (to M.Nishida, M. Nakaya and H.Kurose); from the Institute of Seizon and Life Sciences (to S. Morimoto) and from Naito Foundation and Mochida Memorial Foundation (M. Nishida). M. Hoshijima was supported by NIH (R01 HL081401) and American Heart Association (0840013N).

References

[1] J.A. Towbin, A.M. Lowe, S.D. Colan, et al., Incidence, causes, and outcomes of dilated cardiomyopathy in children, JAMA 296 (2006) 1867-1876.

[2] W.B. Maclellan, A. Lusis, Dilated cardiomyopathy: learning to live with yourself, Nat. Med. 9 (2003) 1455-1456.

[3] E. Grunig, J.A. Tasman, H. Kucherer, et al., Frequency and phenotypes of familial dilated cardiomyopathy, J. Am. Coll. Cardiol. 31 (1998) 186-194.

[4] J.A. Towbin, N.E. Bowles, The failing heart, Nature. insight review articles. 415 (2002) 227-233.

[5] C-K. Du, S. Morimoto, K. Nishii, et al., Knock-in model of dilated cardiomyopathy caused by troponin mutation, Circ. Res. 101 (2007) 185-194.

[6] S. Arber, G. Halder, P. Caroni, Muscle LIM protein, a novel essential regulator of myogenesis, promotes myogenic differentiation, Cell. 79 (1994) 221-231.

[7] S. Arber, J.J. Hunter, J. Ross Jr, et al., MLP-deficient mice exhibit a disruption of cardiac cytoarchitectural organization, dilated cardiomyopathy, and heart failure, Cell. 88 (1997) 393-403.

[8] R. Knöll, M. Hoshijima, H.M. Hoffman, et al., The cardiac mechanical stretch sensor machinery involves a Z-disc complex that is defective in a subset of human dilated cardiomyopathy, Cell. 111 (2002) 943-955.

[9] R. Knöll, S. Kostin, S. Klede, et al., A common MLP (muscle LIM protein) variant is associated with cardiomyopathy, Circ. Res. 106 (2010) 695-704.

[10] R. Yamamoto, H. Akazawa, K. Ito, et al., Angiotensin II type 1a receptor signals are involved in the progression of heart failure in MLP-deficient mice, Circ. J. 71 (2007) 1958-1964.

[11] H.A. Rockman, K.R. Chien, D-J. Choi, et al., Expression of a β-adrenergic receptor kinase 1 inhibitor prevents the development of myocardial failure in gene-targeted mice, Proc. Natl. Acad. Sci. USA. 95 (1998) 7000-7005.

[12] X. Wang, V.C. Culotta, C.B. Klee, Superoxide dismutase protects calcineurin from inactivation, Nature. 383 (1996) 434-437.

[13] H. Toko, H. Takahashi, Y. Kayama, et al., Ca^{2+}/calmodulin-dependent kinase IIδ causes heart failure by accumulation of p53 in dilated cardiomyopathy, Circulation. 122 (2010) 891-899.

[14] C. Maack, T. Kartes, H. Kilter, et al., Oxygen free radical release in human failing myocardium is associated with increased activity of Rac1-GTPase and represents a target for statin treatment, Circulation. 108 (2003) 1567-1574.

[15] C. Montell, G.M. Rubin, Molecular characterization of the Drosophila trp locus: a putative integral membrane protein required for phototransduction, Neuron. 2 (1989) 1313-1323.

[16] M. Nishida, Y. Hara, T. Yoshida, et al., TRP channels: molecular diversity and physiological function, Microcirculation. 13 (2006) 535-550.

[17] M. Nishida, H. Kurose, Roles of TRP channels in the development of cardiac hypertrophy, Naunyn-Schmiedeberg's Arch. Pharmacol. 378 (2008) 395-406.

[18] E.W. Bush, D.B. Hood, P.J. Papst, et al., Canonical transient receptor potential channels promote cardiomyocyte hypertrophy through activation of calcineurin signaling. J. Biol. Chem. 281(2006) 33487-33496.

[19] K. Kuwahara, Y. Wang, J. McAnally, et al., TRPC6 fulfills a calcineurin signaling circuit during pathologic cardiac remodeling, J. Clin. Invest. 116 (2006) 3114-3126.

[20] M. Seth, Z.S. Zhang, L. Mao, et al., TRPC1 channels are critical for hypertrophic

signaling in the heart, Circ Res. 105 (2009) 1023-1030.

[21] N. Onohara, M. Nishida, R. Inoue, et al., TRPC3 and TRPC6 are essential for angiotensin II-induced cardiac hypertrophy. EMBO J. 25 (2006) 5305-5316.

[22] S. Kiyonaka, K. Kato, M. Nishida, et al., Selective and direct inhibition of TRPC3 channels underlies biological activities of a pyrazole compound, Proc. Natl. Acad. Sci. U S A. 106 (2009) 5400-5405.

[23] J. Heineke, H. Ruetten, C. Willenbockel, et al., Attenuation of cardiac remodeling after myocardial infarction by muscle LIM protein-calcineurin signaling at the sarcomeric Z-disc, Proc. Natl. Acad. Sci. USA. 102 (2005) 1655-1660.

[24] M. Nishida, Y. Sato, A. Uemura, et al., $P2Y_6$ receptor-$G\alpha_{12/13}$ signalling in cardiomyocytes triggers pressure overload-induced cardiac fibrosis, EMBO J. 27 (2008) 3104-3115.

[25] M. Nishida, Y. Maruyama, R. Tanaka, et al., $G\alpha_i$ and $G\alpha_o$ are target proteins of reactive oxygen species, Nature. 408 (2000) 492-495.

[26] M. Nishida, K. Watanabe, Y. Sato, et al., Phosphorylation of TRPC6 channels at Thr69 is required for anti-hypertrophic effects of phosphodiesterase 5 inhibition, J. Biol. Chem. 285 (2010) 13244-13253.

[27] T. Fujii, N. Onohara, Y. Maruyama, et al., $G\alpha_{12/13}$-mediated production of reactive oxygen species is critical for angiotensin receptor-induced NFAT activation in cardiac fibroblasts, J. Biol. Chem. 280(2005) 23041-23047.

[28] D. Granfeldt, M. Samuelsson, A. Karlsson, Capacitative Ca^{2+} influx and activation of the neutrophil respiratory burst. Different regulation of plasma membrane-and granule-localized NADPH-oxidase, J. Leukoc. Biol. 71 (2002) 611-617.

[29] D.B. Graham, C.M. Robertson, J. Bautista, et al., Neutrophil-mediated oxidative

burst and host defense are controlled by a Vav-PLCγ2 signaling axis in mice, J. Clin. Invest. 117 (2007) 3445-3452.

[30] J.M. Li, N.P. Gall, D.J. Grieve, et al., Activation of NADPH oxidase during progression of cardiac hypertrophy to failure, Hypertens. 40 (2002) 477-484.

[31] T. Ago, J. Kuroda, J. Pain, et al., Upregulation of Nox4 by hypertrophic stimuli promotes apoptosis and mitochondrial dysfunction in cardiac myocytes, Circ. Res. 106 (2010) 1253-1264.

[32] H. Sumimoto, Structure, regulation and evolution of Nox-family NADPH oxidases that produce reactive oxygen species, FEBS J. 275 (2008) 3249-3277.

[33] M. Nishida, K. Sugimoto, Y. Hara, et al., Amplification of receptor signaling by Ca^{2+} entry-mediated translocation and activation of PLCγ2 in B lymphocytes, EMBO J. 22 (2003) 4677-4688.

[34] T. Numaga, M. Nishida, S. Kiyonaka, et al., Ca^{2+} influx and protein scaffolding via TRPC3 sustain PKCβ and ERK activation in B cells, J. Cell. Sci. 123 (2010) 927-938.

[35] D.B. Zorov, C.R. Filburn, L.O. Klotz, et al., Reactive oxygen species (ROS)-induced ROS release: a new phenomenon accompanying induction of the mitochondrial permeability transition in cardiac myocytes, J. Exp. Med. 192 (2000) 1001-1014.

[36] N.R. Brady, A. Hamacher-Brady, H.V. Westerhoff, et al., A wave of reactive oxygen species (ROS)-induced ROS release in a sea of excitable mitochondria, Antioxid. Redox. Signal. 8 (2006) 1651-1665.

[37] R. Malhotra, K.M. D'Souza, M.L. Staron, et al., $G\alpha_q$-mediated activation of GRK2 by mechanical stretch in cardiac myocytes: the role of protein kinase C, J. Biol. Chem. 285 (2010) 13748-13760.

[38] J.D. Molkentin, J-R. Lu, C.L. Antos, et al., A calcineurin-dependent transcriptional pathway for cardiac hypertrophy, Cell. 93 (1998) 215-228.

[39] R. Passier, H. Zeng, N. Frey, et al., CaM kinase signaling induces cardiac hypertrophy and activates the MEF2 transcription factor *in vivo*, J. Clin. Invest. 105 (2000) 1395-1406.

[40] M.R. Sayen, A.B. Gustafsson, M.A. Sussman, et al., Calcineurin transgenic mice have mitochondrial dysfunction and elevated superoxide production, Am. J. Physiol. Cell Physiol. 284 (2003) C562-570.

Figure legends

Figure 1. Involvement of TRPC3 in CaMKII activation of MLP-deficient hearts. (A) Protein expression levels of respective TRPC channels in wild type (MLP (+/+)) and MLP-deficient (MLP (-/-)) mouse hearts. Hearts were removed from 5 week-old mice. (n=4) **; $P < 0.01$ (B) Typical time course of Ca^{2+} response induced by OAG (15 μM) in the absence (0 mM Ca^{2+}) or presense of extracellular Ca^{2+} (2 mM Ca^{2+}) in isolated MLP (+/+) mouse cardiomyocytes. Cells were treated with Pyr3 (1 μM). (n=10-12) (C) Maximal Ca^{2+} influx-mediated increase in $[Ca^{2+}]_i$ induced by OAG. (D) Effects of pyrazole-3 (Pyr3) on the phosphorylation of CaMKII proteins. (n=6) *; $P < 0.05$.

Figure 2. Inhibition of TRPC3 attenuates left ventricular dysfunction in MLP-deficient mice. Effects of Pyr3 on morphological changes (A-C) and hypertrophic gene expression (D) in MLP (+/+) and MLP (-/-) mouse hearts. (A) H&E-stained mid-transverse LV sections of the hearts isolated from 8 week-old mice. Bars=400 μm (left) and 50 μm (right). (n=5-11) (B) Heart weight (HW) to body weight (BW) ratios. (C) Average areas of cardiomyocytes. (n=5). (D) Expressions of β-MHC, α-SKA and ACE mRNAs. (n=4). *; $P < 0.05$. **; $P < 0.01$.

Figure 3. Inhibition TRPC3 attenuates interstitial fibrosis of MLP-deficient mice. (A) LV sections stained by picrosirius red (Bars=50 μm). (B) Results of fibrosis in MLP (-/-) and MLP (+/+) mouse hearts with or without Pyr3. (n=5) (C) Effects of Pyr3 on the expressions of ACE, periostin, and GAPDH proteins. (n=6) *; $P < 0.05$,

**; $P < 0.01$.

Figure 4. TRPC3 mediates mechanical stretch-induced superoxide production in cardiomyocytes. (A) Immunostaining for 4-HNE adducts of the hearts. (B) Superoxide production of the hearts stained by DHE. Bars=50 μm. (n=5) (C) Effects of Pyr3 on the expression and activity of Rac1 in MLP (-/-) and MLP (+/+) mouse hearts. n.s.; not significant. (n=6) (D) Average time courses of increase in DCF fluorescence intensity induced by mechanical stretch in rat neonatal cardiomyocytes. Cardiomyocytes were treated with Pyr3 (1 μM) 30 min before mechanical stretch. (E, F) Effects of Pyr3 on the OAG-induced ROS production in rat cardiomyocytes. (E) Typical images of DHE accumulation and (F) average increases in DHE fluorescence intensity. Cells were treated with Pyr3 (1 μM) or DPI (1 μM) for 20 min before the addition of OAG (30 μM). Ten min after OAG stimulation, cells were loaded with DHE (2 μM) at 37℃ for 1 h. Bars=50 μm. (n=34-63) *; $P < 0.01$, **; $P < 0.001$.

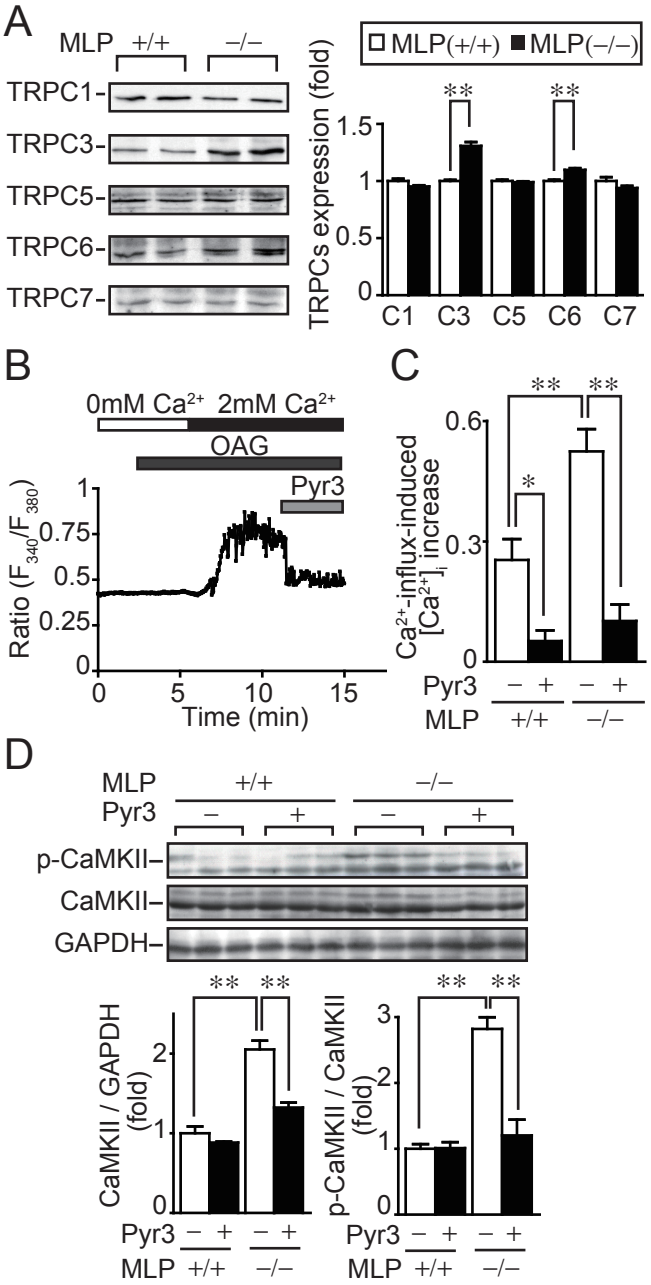

Figure 1. Kitajima *et al*.

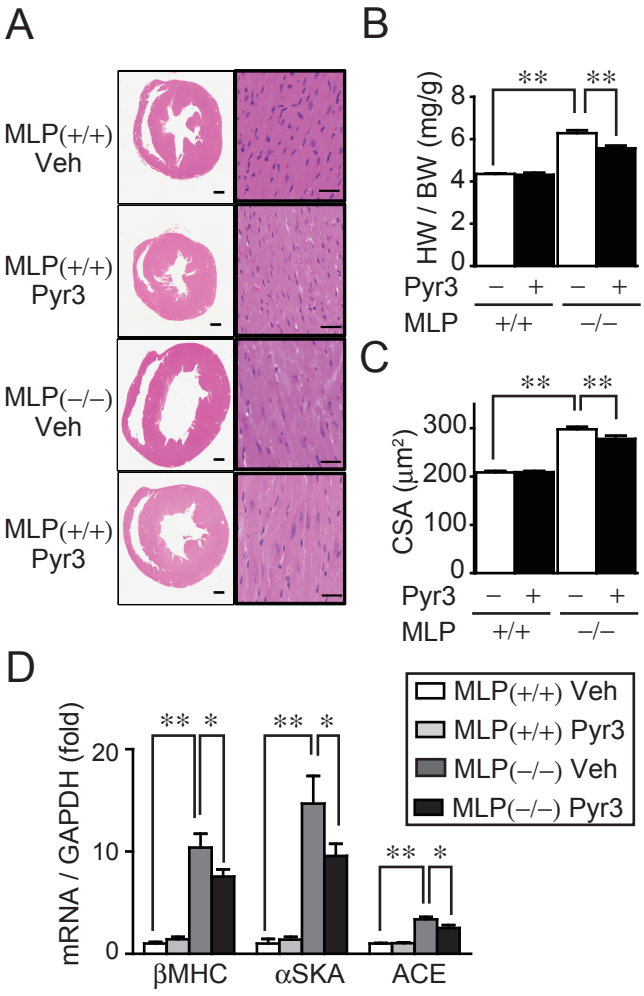

Figure 2. Kitajima *et al*.

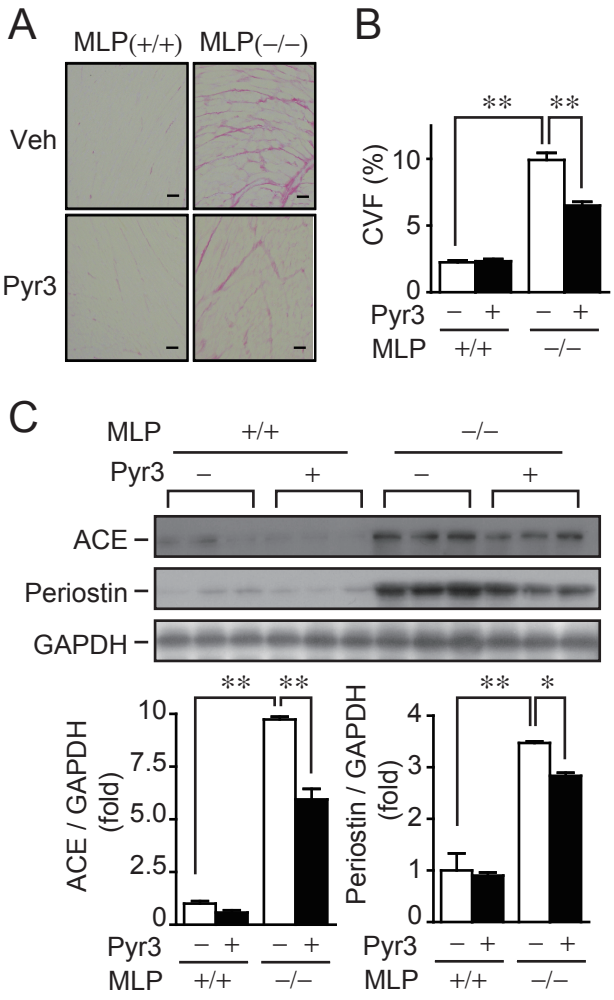

Figure 3. Kitajima *et al*.

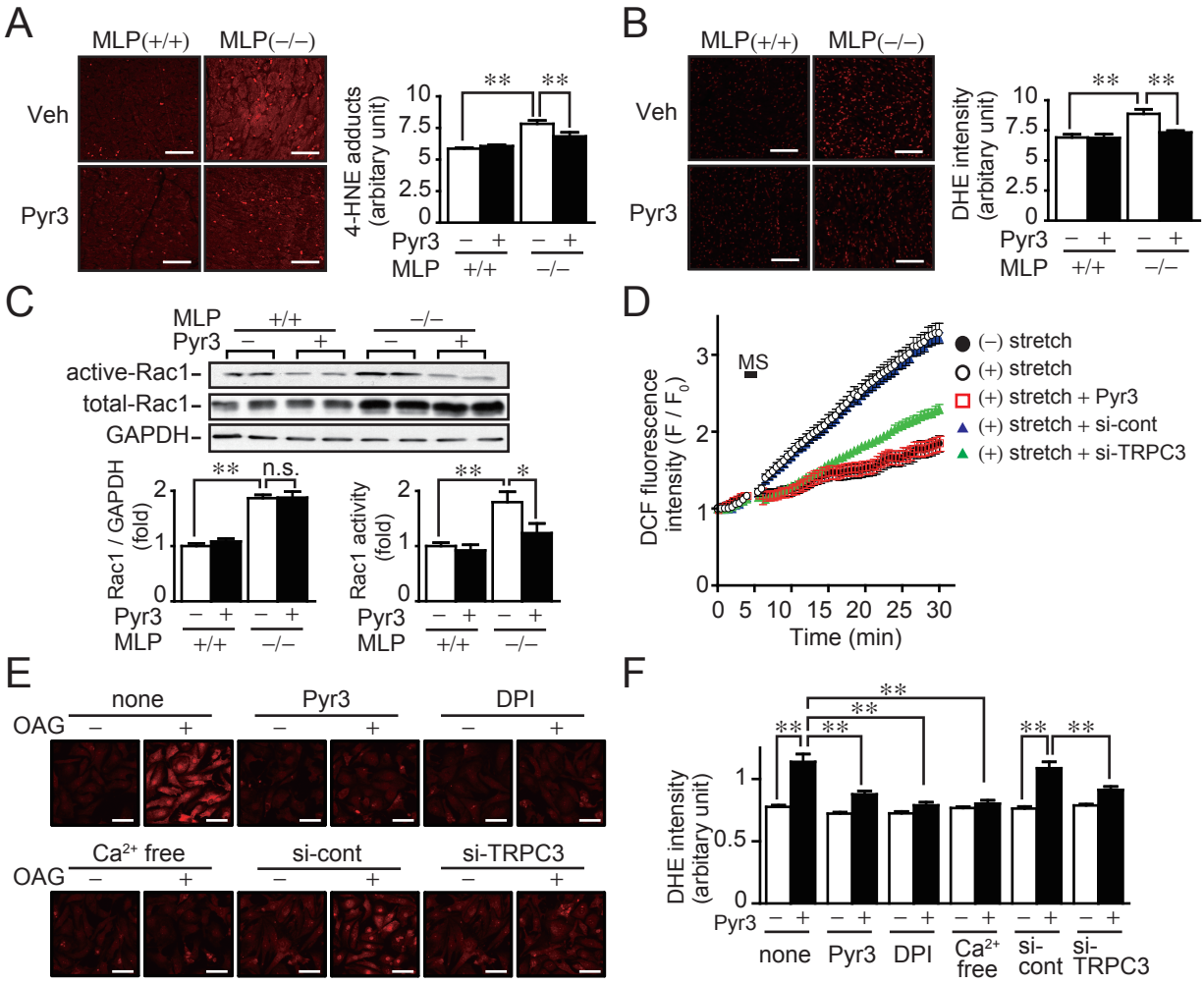

Figure 4. Kitajima *et al*.

Table 1 Echocardiographic parameters

	$MLP^{(+/+)}$ Veh (n=5)	$MLP^{(+/+)}$ Pyr3 (n=5)	$MLP^{(-/-)}$ Veh (n=11)	$MLP^{(-/-)}$ Pyr3 (n=11)
HR (bpm)	538 ± 10	541 ± 14	533 ± 11	529 ± 16
IVSd (mm)	0.88 ± 0.04	0.90 ± 0.03	0.63 ± 0.03**	0.92 ± 0.04##
LVPWd (mm)	0.98 ± 0.02	0.94 ± 0.02	0.71 ± 0.04**	0.97 ± 0.04##
LVIDd (mm)	2.08 ± 0.09	2.04 ± 0.02	3.25 ± 0.17**	2.64 ± 0.04##
LVIDs (mm)	0.50 ± 0.06	0.48 ± 0.02	2.48 ± 0.19**	1.39 ± 0.18##
EF (%)	98.8 ± 0.3	98.8 ± 0.2	56.0 ± 3.9**	83.2 ± 3.4##
FS (%)	78.0 ± 2.1	78.0 ± 1.1	25.4 ± 1.1**	50.6 ± 4.7##

HR, heart rate; IVSd, interventricular septum diastolic diameter; LVPWd, left ventricular posterior wall diastolic diameter; LVIDd, left ventricular internal at end-diastole; LVIDs, left ventricular internal diameters at end-systole; EF, ejection fraction; FS, Fractional shortening; Veh, vehicle; *P < 0.05, **P < 0.01 vs $MLP^{(+/+)}$ Veh, and #P < 0.05, ##P < 0.01 vs $MLP^{(-/-)}$ Veh.

Table 2 Cardiac parameters measured by Millar Catheter

	$MLP^{(+/+)}$ Veh (n=5)	$MLP^{(+/+)}$ Pyr3 (n=5)	$MLP^{(-/-)}$ Veh (n=11)	$MLP^{(-/-)}$ Pyr3 (n=11)
Heart Rate (bpm)	498 ± 3	504 ± 2	500 ± 4	505 ± 1
LVESP (mmHg)	123 ± 4	127 ± 3	102 ± 2**	108 ± 2#
LVEDP (mmHg)	4.4 ± 0.8	3.6 ± 1.0	14.1 ± 1.2**	8.4 ± 0.4##
dP/dt max (mmHg/sec)	13365 ± 199	12756 ± 412	6252 ± 294**	8235 ± 316##
dP/dt min (mmHg/sec)	8049 ± 617	8444 ± 530	3240 ± 185**	4516 ± 178##
tau (msec)	9.8 ± 0.4	8.9 ± 0.2	28.7 ± 1.8**	20.2 ± 0.8##

HR, heart rate; LVESP, left ventricular end systolic pressure; LVEDP, left ventricular end diastolic pressure;
dP/dt max, maximal rate of pressure development; dP/dt min, maximal rate of decay of pressure; tau, monoexponential time constant of relaxation.
Veh, vehicle; *P < 0.05, **P < 0.01 vs $MLP^{(+/+)}$ Veh, and #P < 0.05, ##P < 0.01 vs $MLP^{(-/-)}$ Veh